

Ferromagnetism in a periodic Anderson-like organic polymer at half-filling and zero temperature

W. Z. Wang*

Department of Physics, Wuhan University, Wuhan 430072, People's Republic of China

(Received 22 September 2005; revised manuscript received 30 November 2005; published 13 January 2006)

We have studied the ground state of a quasi-one-dimensional periodic Anderson-like chain with the f orbitals connected only to the conduction orbitals at the even sites. Using the exact diagonalization (ED) technique and the Hartree-Fock approximation (HFA), we find that at half-filling, for the symmetric case, the ground state is always ferrimagnetic. In the weak hybridization case, the ferromagnetism is mainly contributed by the local magnetic moment on the f orbital while in the strong hybridization case, the ferromagnetism mainly results from the ferromagnetic correlation between the conduction orbitals. In the large-hybridization limit, the conduction orbitals at the odd sites form a spin- $\frac{1}{2}$ ferromagnetic chain with exchange decoupling from another conduction orbital and the f orbital. For the asymmetric case, we construct the phase diagram. The region between two critical values of the energy of the f orbital is the ferrimagnetic state. Outside this region, the ground state is antiferromagnetic. This region depends on the on-site Coulomb repulsion on the f orbital and the hybridization. In the large-hybridization limit, the ferrimagnetic state exists only in the symmetric case. The results by the HFA and the ED are consistent quantitatively in the weak coupling and strong hybridization case.

DOI: 10.1103/PhysRevB.73.035118

PACS number(s): 71.27.+a, 75.30.Fv, 71.10.Fd

I. INTRODUCTION

The microscopic mechanism of itinerant ferromagnetism is a long-standing problem in strongly correlated electron systems. The Hubbard model was introduced in 1963 to describe ferromagnetism in such systems.¹ Unfortunately, very few rigorous results are available. Nagaoka² showed that when a single hole is introduced into the just half-filled system, the ground state is a completely polarized ferromagnetic state in the strong coupling regime. With a bipartite lattice and a half-filled band, Lieb³ obtained the ground state with spin $S = (|A| - |B|)/2$, where $|B|$ ($|A|$) is the number of sites in the B (A) sublattice. For a system with a magnetic impurity embedded in a conducting host, the Anderson model⁴ has been successfully applied to describe the physics.

For lattice systems, the natural extension of the impurity Anderson model is the periodic Anderson model (PAM). The magnetism in this model has been studied extensively. The rigorous results show that the ground state of the PAM is a singlet at half-filling⁵ and exhibits short-range antiferromagnetic correlations.⁶ A variety of numerical techniques have been applied to the PAM. The magnetic correlation of the nonmagnetic ground state and the lowest excitation were studied by the exact diagonalization (ED) techniques for short PAM chains.^{7,8} The spectral-weight function of the lattice Anderson model on small square and tetrahedral clusters was also investigated by the ED (Ref. 9). Quantum Monte Carlo (QMC) simulations¹⁰ have shown that the local f -electron spins are compensated with other f electrons as well as band electrons leading to a singlet ground state. The results of QMC also show that the nonsaturated ferromagnetism of the PAM can be interpreted by a mechanism for itinerant ferromagnetism based on a simple two-band model.¹¹ Numerical studies of finite chains employing the density matrix renormalization group (DMRG) have provided the phase diagram of the one-dimensional^{12,13} PAM. For strong coupling, the quarter-filled system has a $S=0$

ground state with strong antiferromagnetic correlations. At slightly larger fillings there is a transition to a ferromagnetic state. For the symmetric and asymmetric Anderson lattices at half-filling, the charge gap, the spin gap, and the quasiparticle gap have been studied by the DMRG technique.¹⁴ For the electron density between half and three-quarters fillings, a ferromagnetic ground state of the one-dimensional PAM has been found exactly in the strong hybridization and strong coupling regime.¹⁵ Recently, the ground-state properties of the symmetric and asymmetric one-dimensional PAM as a function of band filling and the model parameters have been studied by the local mean-field approach.¹⁶ The phase diagram for both cases was obtained and the local moment and occupation number of the f level were calculated.

In this paper, we consider another simplified structure of a quasi-one dimensional organic polymer¹⁷ *poly*-BIPO schematically shown in Fig. 1. The main zigzag chain consists of carbon atoms. R denotes side radical with unpaired electron. This model has been described by a Peierls-Hubbard model¹⁸ with the on-site Coulomb interaction U independent of site. The ferrimagnetic ground state was obtained by the Hartree-Fock approximation¹⁸ (HFA). Since this structure is a bipartite lattice, Lieb's theorem also gives the ground state with spin $S = \frac{1}{2}$ per unit cell for the Hubbard model at half-filling. For a generalized symmetric Hubbard model with the hopping t_{ij} and the on-site Coulomb interaction U_i to be site dependent, the rigorous result¹⁹ also shows that the ground state of this bipartite lattice has the ferrimagnetic long-range ordering. However, for the asymmetric case in which the orbital energy ϵ_i is not equal to $-U_i/2$, above rigorous theo-

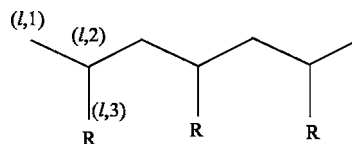


FIG. 1. A quasi-one-dimensional organic polymer chain.

rems are not applicable and the ground state is not known. The aim of this work is to study the properties of the ground state for a special asymmetric case in which there are an uncorrelated conduction orbital at each site in the zigzag chain and a correlated localized f orbital at each side site R . In this periodic Anderson-like model (PALM), the localized orbital hybridizes with the conduction orbital at the even site. Using the ED technique and the HFA, we study the phase diagram of the present PALM at zero temperature and half-filling, the spin correlation and the charge fluctuations in different ground-state phases. Our calculation shows that in the symmetric case, the ground state is always ferrimagnetic. This result indicates that the rigorous result in Ref. 19 is also true for the on-site Coulomb repulsion $U_i=0$ at sites of the main chain. For the asymmetric case, the ferrimagnetic state exists in a region of the energy ϵ_f of the localized orbital, which depends on the on-site Coulomb interaction at the localized orbital and the hybridization strength. For weak coupling and strong hybridization, the phase diagram by both methods is consistent.

The remainder of this paper is organized as follows. The model and the computational method are given in Sec. II. The phase diagrams and spin correlations are described in Sec. III. Finally the discussion and conclusion are given.

II. MODEL AND COMPUTATIONAL METHOD

The Hamiltonian for the quasi-one-dimensional periodic Anderson-like chain in Fig. 1 is defined by

$$H = -t \sum_{l,\sigma} (c_{l,1,\sigma}^\dagger c_{l,2,\sigma} + c_{l+1,1,\sigma}^\dagger c_{l,2,\sigma} + \text{H.c.}) + \epsilon_f \sum_{l,\sigma} n_{l,3,\sigma} + U \sum_l n_{l,3,\uparrow} n_{l,3,\downarrow} + V \sum_{l,\sigma} (c_{l,2,\sigma}^\dagger c_{l,3,\sigma} + \text{H.c.}). \quad (1)$$

Here, $c_{l,i,\sigma}^\dagger$ ($c_{l,i,\sigma}$) are the creation (annihilation) operators of electron with spin $\sigma = \uparrow, \downarrow$ on the i th site of the l th cell, respectively. $n_{l,i,\sigma}$ is the number operator of electron. In the notation (l, i) , $i=1, 2$ denotes the conduction orbitals on the zigzag chain while $i=3$ denotes the localized f orbitals at side site R . t is the hopping integral between the nearest-neighbor conduction orbitals, ϵ_f is the energy of the localized f orbital, U is the on-site Coulomb repulsion of the f electrons, and V is the hybridization between the localized orbital and conduction orbital. In the following discussion, we take t as energy unit.

Within the ED method,²⁰ the calculation is performed in a subspace with a given number of electrons N and a given z component S_z of the total spin \mathbf{S} of the system. In order to determine quantum number S of the total spin of the ground state, we calculate the mean value of the operator \mathbf{S}^2 in the ground state with the lowest possible S_z (0 or $\frac{1}{2}$ according to whether N is even or odd). Since $\langle \mathbf{S}^2 \rangle = S(S+1)$, we can deduce the value of S . The ground-state phases are characterized through the local spin-spin correlations $\langle \mathbf{S}_{l,i} \cdot \mathbf{S}_{m,j} \rangle$ and spin structure factor $S(q)$

$$S(q) = \frac{1}{N^2} \sum_{li,mj} e^{iq(l-m)} \langle \mathbf{S}_{l,i} \cdot \mathbf{S}_{m,j} \rangle. \quad (2)$$

Within the HFA, we treat the electron-electron interaction in the HFA,

$$n_{l,i,\uparrow} n_{l,i,\downarrow} = \langle n_{l,i,\uparrow} \rangle n_{l,i,\downarrow} + \langle n_{l,i,\downarrow} \rangle n_{l,i,\uparrow} - \langle n_{l,i,\uparrow} \rangle \langle n_{l,i,\downarrow} \rangle. \quad (3)$$

Here, $\langle \rangle$ is the average with respect to the mean-field-theory ground state. Due to translation symmetry, $\langle n_{l,i,\sigma} \rangle = \langle n_{i,\sigma} \rangle$ is independent of l .

In order to diagonalize the Hamiltonian, we take the Fourier transformation of $c_{l,i,\sigma}$,

$$c_{l,i,\sigma} = N_c^{-1/2} \sum_k e^{-ikl} b_{k,i,\sigma}. \quad (4)$$

Here, N_c is the number of unit cell. Then the Hamiltonian becomes

$$H = \sum_{k,\sigma} \mathbf{b}_{k,\sigma}^\dagger \mathbf{M}^\sigma(k) \mathbf{b}_{k,\sigma}. \quad (5)$$

Here, $\mathbf{b}_{k,\sigma}^\dagger$ is a three-dimensional row vector defined as,

$$\mathbf{b}_{k,\sigma}^\dagger = (b_{k,1,\sigma}^\dagger, b_{k,2,\sigma}^\dagger, b_{k,3,\sigma}^\dagger). \quad (6)$$

$\mathbf{M}^\sigma(k)$ is a 3×3 energy matrix

$$\mathbf{M}^\sigma(k) = \begin{pmatrix} 0 & -1 - e^{-ik} & 0 \\ -1 - e^{ik} & 0 & V \\ 0 & V & U \langle n_{3,-\sigma} \rangle + \epsilon_f \end{pmatrix}. \quad (7)$$

Here, $-\sigma$ denotes down spin (up spin) if σ is up spin (down spin). From the equation

$$\mathbf{M}^\sigma(k) \mathbf{V}_{i\sigma}(k) = E_{i,\sigma}(k) \mathbf{V}_{i\sigma}(k), \quad (i=1, 2, 3), \quad (8)$$

we can get an eigenvalue $E_{i,\sigma}(k)$ and an eigenvector $\mathbf{V}_{i\sigma}(k)$ of the matrix $\mathbf{M}^\sigma(k)$, where $i (=1, 2, 3)$ is the energy-band index. The unitary transformation $\mathbf{P}^\sigma(k)$ that diagonalizes $\mathbf{M}^\sigma(k)$ is given by

$$\mathbf{P}^\sigma(k) = [\mathbf{V}_{1\sigma}(k), \mathbf{V}_{2\sigma}(k), \mathbf{V}_{3\sigma}(k)]. \quad (9)$$

So we can define an three-dimensional new operator $\mathbf{a}_{k,\sigma}^\dagger = \mathbf{b}_{k,\sigma}^\dagger \mathbf{P}^\sigma(k)$ to diagonalize the Hamiltonian Eq. (5),

$$H = \sum_{k,\sigma} \sum_{i=1}^3 E_{i,\sigma}(k) a_{k,i,\sigma}^\dagger a_{k,i,\sigma}. \quad (10)$$

Here, $a_{k,i,\sigma}^\dagger$ is the i th component of $\mathbf{a}_{k,\sigma}^\dagger$. The ground state can now be written as

$$|G\rangle = \prod_{k,i,\sigma}^{(occ)} a_{k,i,\sigma}^\dagger |0\rangle. \quad (11)$$

Here, $|0\rangle$ is electron vacuum state and (occ) labels the states occupied by electrons. From Eq. (11), we can get the charge density

$$\langle n_{j,\sigma} \rangle = N_c^{-1} \sum_{k,i,\sigma}^{(occ)} V_{ji\sigma}(k) V_{ji\sigma}^*(k). \quad (12)$$

Here, $V_{ji\sigma}(k)$ is the j th component of the eigenvector $\mathbf{V}_{i\sigma}(k)$.

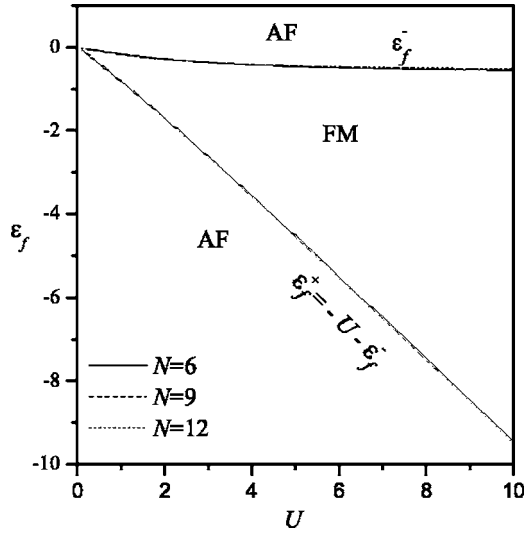


FIG. 2. The phase diagram by the ED for $V=0.1$ and different system size N .

Because the matrix $\mathbf{M}^\sigma(k)$ contains the term $\langle n_{j,\sigma} \rangle$, we must solve Eqs. (8) and (12) self-consistently. The spin density $\langle S_j^z \rangle$ is defined as

$$\langle S_j^z \rangle = \frac{1}{2} (\langle n_{j,\uparrow} \rangle - \langle n_{j,\downarrow} \rangle). \quad (13)$$

III. RESULTS AND DISCUSSION

We first study the phase diagram of the quasi-one-dimensional periodic Anderson-like chain at half-filling. We use the ED technique to calculate the quantity \mathbf{S}^2 in the ground state and obtain the value of S . Although the ED can only deal with a small system, for the one-dimensional interacting system such as the PAM and the Kondo lattice,^{7,21} the magnetic correlation and phase diagram have been determined accurately on the basis of the precise treatments of the finite-size effects observed in the ED data. Figure 2 shows the phase diagram for the weak hybridization $V=0.1$ and for the cluster with the size $N=6, 9$, and 12 under periodic boundary condition. The region between two curves is the ferrimagnetic (FM) phase with the spin $S=\frac{1}{2}$ per unit cell. Outside this region, the ground state is the antiferromagnetic (AF) phase. We will discuss the properties of the two ground-state phases later. It is obvious that the phase diagrams for these three sizes are nearly the same and the finite-size effect is very small. In the case of the symmetric Hubbard model, the rigorous result¹⁹ shows that the ground state of this bipartite lattice has the spin $\frac{1}{2}$ per unit cell. Our result indicates that the ferrimagnetic ground state exists in a much larger region of parameter space, e.g., for the asymmetric case $\epsilon_f \neq -U/2$ and for the on-site Coulomb $U_i=0$ at sites on the main chain. The calculated result shows that the two boundaries ϵ_f^- and ϵ_f^+ between the FM phase and AF phase have the relation $\epsilon_f^+ = -U - \epsilon_f^-$, which can also be induced from the analysis of the symmetry of the Hubbard Hamiltonian for bipartite lattice.²² Hence, in the following discus-

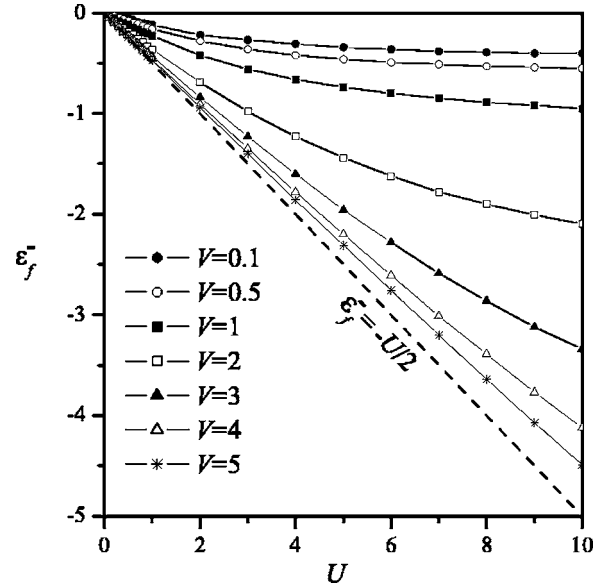


FIG. 3. The upper critical point ϵ_f^- as a function of U for different V . The dashed line corresponds to the symmetric case $\epsilon_f^- = -U/2$.

sion, we just analyze the behavior of the upper critical point ϵ_f^- .

As the hybridization V increases, the region of the FM phase becomes smaller. Figure 3 shows the critical point ϵ_f^- as a function of U for different V and the cluster size $N=12$. One can see that as V increases, ϵ_f^- approaches gradually to the value $-U/2$. This result means that for the symmetric PALM, the ground state is always ferrimagnetic. In order to exhibit the nature of the phase transition, we have performed the calculation of the energy band by the HFA. We solve Eqs. (8) and (12) self-consistently and obtain the band spectra and the spin density. Figure 4 shows the energy bands for $U=2$, $\epsilon_f=-0.8$, $V=0.1$ and 2 . The Coulomb repulsion U and the hybridization V remove the degeneracy in the spin configuration. In the ground state, the lowest two up-spin bands and one down-spin band are occupied. Hence the ground state is ferrimagnetic and has the spin $S=\frac{1}{2}$ per unit cell. In this case, from Eq. (8) one can find that the Fermi level is exactly at $E_{3,\sigma}(k=\pi)=0$. We can get the necessary condition for the FM phase from this fact. In the small- V limit, we have

$$E_{1,\sigma}(\pi) \approx a_\sigma + \frac{V^2}{a_\sigma}, \quad E_{2,\sigma}(\pi) \approx -\frac{V^2}{a_\sigma}, \quad E_{3,\sigma}(\pi) = 0. \quad (14)$$

Here, $a_\sigma = U \langle n_{3,-\sigma} \rangle + \epsilon_f$. Under the condition $a_\uparrow < 0$ and $a_\downarrow > 0$, in Fig. 4(a) the bands $E_{1,\uparrow}$, $E_{3,\uparrow}$, and $E_{2,\downarrow}$ are filled and the FM phase is stable. This condition induces

$$-U \langle n_{3,\downarrow} \rangle > \epsilon_f > -U \langle n_{3,\uparrow} \rangle. \quad (15)$$

Because the charge density $\langle n_{3,\sigma} \rangle$ is between 0 and 1, Eq. (15) leads to $0 > \epsilon_f > -U$. In the large- V limit, we have

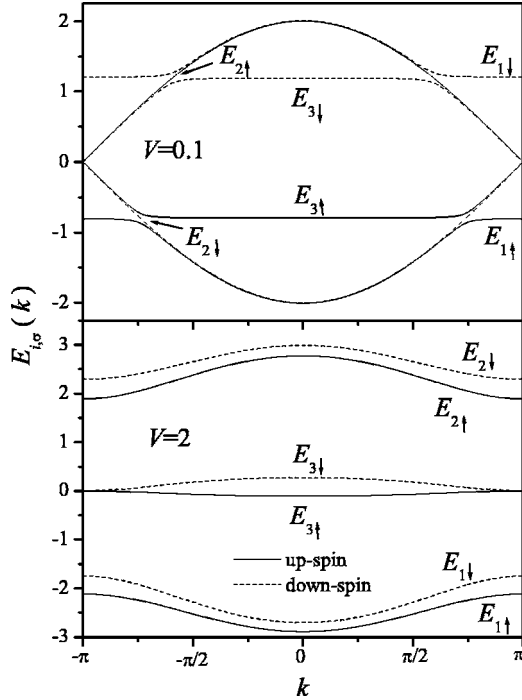


FIG. 4. The energy band $E_{i,\sigma}(k)$ for $U=2$, $\epsilon_f = -0.8$, $V=0.1$ and 2.

$$E_{1,\sigma}(k) \approx -V + \frac{a_\sigma}{2}, \quad E_{2,\sigma}(k) \approx V + \frac{a_\sigma}{2},$$

$$E_{3,\sigma}(k) \approx \frac{2(1 + \cos k)a_\sigma}{V^2}. \quad (16)$$

In this case, there is almost no dispersion in the band structure. The splits of the bands with respect to spin are much smaller than those for small V . One can find this tendency in Fig. 4(b) for the strong hybridization $V=2$. To stabilize the FM state, one also needs the condition $a_\uparrow < 0$ and $a_\downarrow > 0$, under which the bands $E_{1,\uparrow}$, $E_{3,\uparrow}$, and $E_{1,\downarrow}$ are filled. This condition also leads to Eq. (15). In the intermediate hybridization case, the numerical calculation shows that the FM state also requires this condition.

As the hybridization V is very small and the f level ϵ_f is just below the Fermi level $E_F=0$, due to the Coulomb repulsion U the f orbital is nearly singly occupied by up-spin electrons. The flat parts of the bands $E_{3,\uparrow}$ and $E_{1,\uparrow}$ in Fig. 4(a) are almost occupied by the electrons on the f orbital. The ferromagnetism is mainly contributed by the magnetic moment on the localized f orbital. In this case, the charge density $\langle n_{3,\uparrow} \rangle \rightarrow 1$ and $\langle n_{3,\downarrow} \rangle \rightarrow 0$. From Eq. (15), we know that the size of the upper critical point $\bar{\epsilon}_f^-$ is very small. As V is enhanced, $\langle n_{3,\uparrow} \rangle$ decreases and $\langle n_{3,\downarrow} \rangle$ increases so that the size of the $\bar{\epsilon}_f^-$ increases. In the large- V limit, the f orbital is nearly doubly occupied. The charge densities $\langle n_{3,\uparrow} \rangle$ and $\langle n_{3,\downarrow} \rangle$ are close to $\frac{1}{2}$. In this case, from Eq. (15) one can see that the upper critical $\bar{\epsilon}_f^-$ approaches to $-U/2$. Therefore, the ferromagnetism in the FM state is mainly contributed by the magnetic moment on the zigzag chain. The above discussion

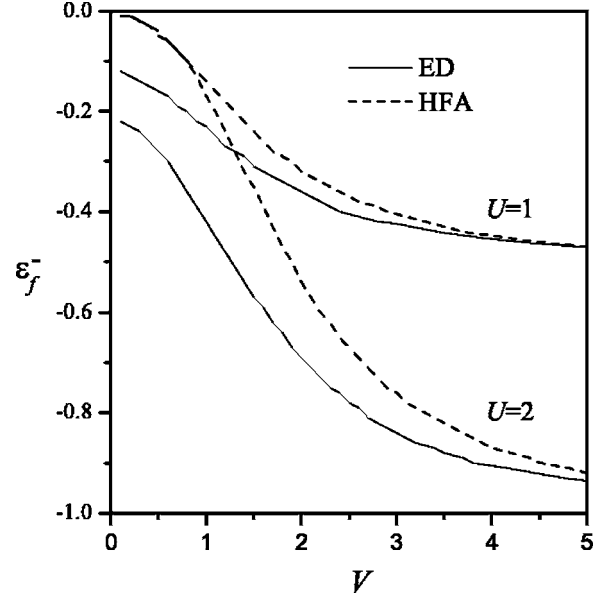


FIG. 5. The upper critical point $\bar{\epsilon}_f^-$ by the ED and the HFA as a function of V for different U .

based on the HFA is consistent with the phase diagram in Fig. 3 obtained by the ED technique. To check the applicability of the HFA, in Fig. 5 we give a comparison of the phase diagrams by the HFA and the ED. Although the tendency of the phase diagrams by both methods is similar, the quantitative consistency only occurs for small Coulomb repulsion U and large hybridization strength V .

In order to exhibit the properties of the ground-state phases, we study the spin-spin correlations by the ED with the cluster size $N=12$. Figure 6(a) shows the spin structure factor $S(q)$ defined in Eq. (2) for $U=5$, $V=0.5$, and different ϵ_f . For $\epsilon_f = -0.6$, $S(q)$ has a peak at $q=0$ and the ground state is ferrimagnetic. For $\epsilon_f = -0.4$, the AF phase is clearly identified with a peak of $S(q)$ at $q=\pi$. Figure 6(b) shows the size dependence of the peak weight $S(q=0)$ and $S(q=\pi)$ in the two phases for the cluster size $N=6, 9$, and 12. To extrapolate to the thermodynamic limit, the FM state exhibits long-range order since the total spin is $S=\frac{1}{2}$ per unit cell for any size. In the AF state, $S(q=\pi)$ decreases with the cluster sizes but is also nonzero in the thermodynamic limit. This behavior may indicate a long-range antiferromagnetic correlation, which is in contrast to the short-range antiferromagnetic correlation in the standard⁶ PAM. In the symmetric Hubbard model, the rigorous result¹⁹ shows that the ground state of this bipartite lattice has both the ferromagnetic and antiferromagnetic long-range orderings. In the asymmetric case, the transition between the FM state and the AF state results from the competition between these two correlations.

The local spin-spin correlations $\langle \mathbf{S}_{l,i} \cdot \mathbf{S}_{m,j} \rangle$ as functions of the hybridization V are shown in Fig. 7 for $\epsilon_f = -1$, $U=2, 5$, and 10. The double occupancy $W_i = \langle n_{i,\uparrow} n_{i,\downarrow} \rangle$ is also given in Fig. 8 for the same parameters. In the symmetric case $U=2$, the ground state is always ferrimagnetic. As the hybridization V is very small, there are no double occupancies on the f orbital and a large double occupancy on the conduction orbital. Hence the ferromagnetic correlation $\langle \mathbf{S}_{l,3} \cdot \mathbf{S}_{l+1,3} \rangle$

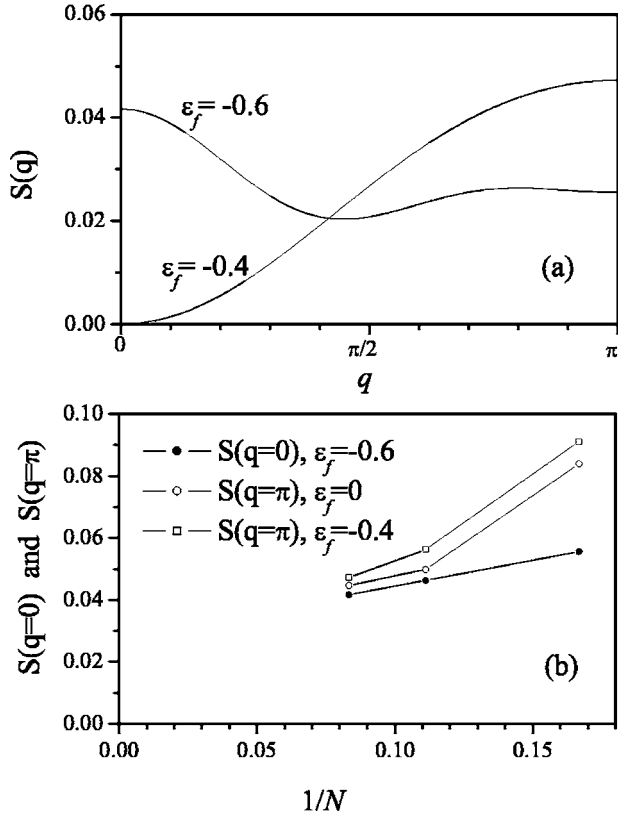


FIG. 6. (a) Spin structure factor $S(q)$ for $U=5$, $V=0.5$, and different ϵ_f . (b) The size dependence of the peak weight $S(q=0)$ and $S(q=\pi)$ in the two phases for the cluster size $N=6, 9$, and 12 .

between two highly localized f orbitals almost has the saturation value 0.25. The appropriate antiferromagnetic correlations between the nearest-neighboring orbitals (including both the conduction orbital and the localized f orbital) play an important role in mediating this ferromagnetic correlation. For small V , the ferromagnetism mainly results from the localized magnetic moment on the f orbital. With increasing V , the double occupancy on the f orbital increases while that on the conduction orbital $(l, 1)$ decreases. As V is very large, the conduction orbital $(l, 1)$ is nearly singly occupied while the f orbital is occupied almost equally by up-spin and down-spin electrons. As a result, the ferromagnetic correlation between two conduction orbitals $(l, 1)$ and $(l+1, 1)$ reaches to the saturation value 0.25 while the spin correlation between two f orbitals nearly vanishes. This result shows that in the large- V limit and the symmetric case, the conduction orbitals $(l, 1)$ form a spin- $\frac{1}{2}$ ferromagnetic chain with exchange decoupling from the conduction orbitals $(l, 2)$ and the f orbitals because the spin correlations $\langle \mathbf{S}_{l,1} \cdot \mathbf{S}_{l,2} \rangle$, $\langle \mathbf{S}_{l,3} \cdot \mathbf{S}_{l+1,3} \rangle$ and $\langle \mathbf{S}_{l,2} \cdot \mathbf{S}_{l+1,2} \rangle$ nearly vanish. Meanwhile, $\langle \mathbf{S}_{l,2} \cdot \mathbf{S}_{l,3} \rangle$ shows a strong antiferromagnetic correlation between the conduction orbitals $(l, 2)$ and f orbital but does not reach the saturation value -0.75 of a singlet because these two orbitals are partially doubly occupied.

In the asymmetric case for $U=5, 10$, and small V , the ground state is the FM phase. As V increases to a critical value V_c corresponding to the jumps in Figs. 7 and 8, the ground state is the AF phase. In the AF phase, for weak

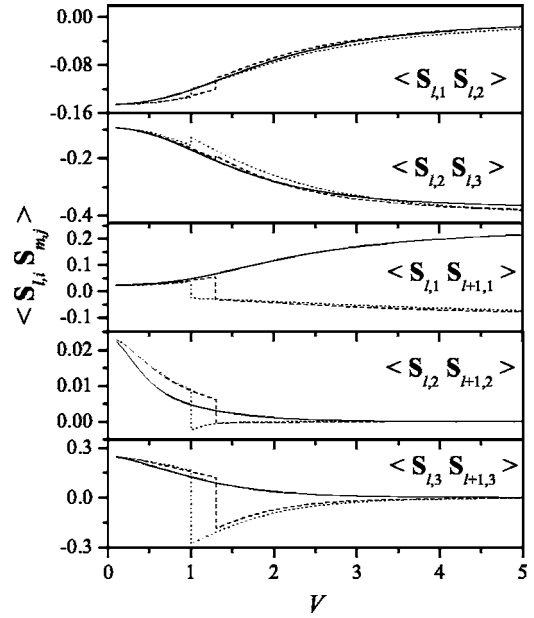


FIG. 7. The spin-spin correlations $\langle \mathbf{S}_{l,i} \cdot \mathbf{S}_{m,j} \rangle$ as a function of V for $\epsilon_f = -1$, $U=2$ (solid), 5 (dashed), and 10 (dotted).

hybridization the f orbital is mainly singly occupied and there is a strong antiferromagnetic correlation between two f orbitals. For strong hybridization, the spin correlations $\langle \mathbf{S}_{l,1} \cdot \mathbf{S}_{l,2} \rangle$, $\langle \mathbf{S}_{l,3} \cdot \mathbf{S}_{l+1,3} \rangle$, and $\langle \mathbf{S}_{l,2} \cdot \mathbf{S}_{l+1,2} \rangle$ tend to zero while the antiferromagnetic correlation $\langle \mathbf{S}_{l,2} \cdot \mathbf{S}_{l,3} \rangle$ reaches a large value. Similarly to the symmetric case, it seems that the conduction orbital $(l, 1)$ also has exchange decoupling from the conduction orbitals $(l, 2)$. However, the spin correlation between two conduction orbitals $(l, 1)$ and $(l+1, 1)$ is much smaller than that of a spin- $\frac{1}{2}$ antiferromagnetic chain because the double occupancy on the conduction orbital $(l, 1)$ is large.

In Fig. 9, we show the charge density $\langle n_i \rangle = \langle n_{i,\uparrow} \rangle + \langle n_{i,\downarrow} \rangle$ as a function of the hybridization V for $\epsilon_f = -1$, $U=2, 5$, and 10 . In the symmetric case $U=2$ and $\epsilon_f = -1$, the ground state is ferrimagnetic and there is no charge fluctuation due to particle-hole symmetry. In the asymmetric case $U=5$ and 10 , with increasing V , the charge density transfers from the f orbital to the conduction orbitals. Because for small V the f orbital is nearly singly occupied by an up-spin electron, the reduction of charge density on the f orbital leads to the decreasing of the ferromagnetic correlation between two f orbitals in Fig. 7. As V increases to a critical value V_c , the FM state transits to the AF state. Let us analyze the mechanism of the transition. From Fig. 9, one can find that at the critical value V_c there is an abrupt drop and jump in charge density on the f orbital and the conduction orbitals, respectively. The abrupt jump in charge density on the conduction orbitals $(l, 1)$ induces a large increase of double occupancy on this orbital in Fig. 8. Hence, there is a large reduction in the antiferromagnetic correlation between the nearest-neighboring conduction orbitals $(l, 1)$ and $(l, 2)$. On the other hand, the drop in charge density on the f orbital weakens the antiferromagnetic correlation between the f orbital and the conduction orbitals $(l, 2)$. In the FM state, these two kinds of

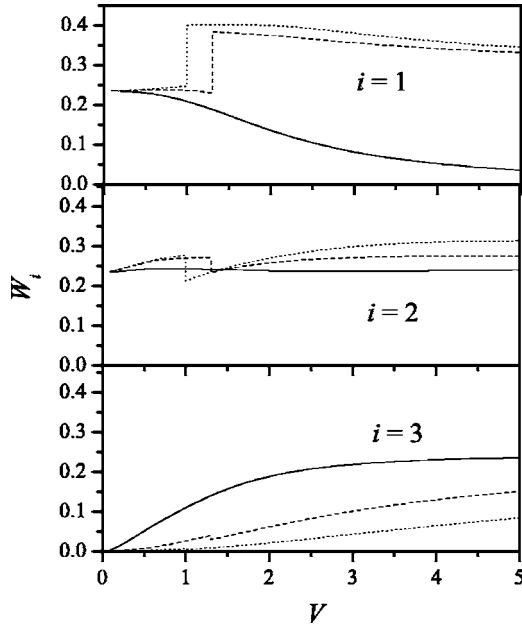


FIG. 8. The double occupancy $W_i = \langle n_{i,\uparrow} n_{i,\downarrow} \rangle$ at site (l,i) for the same parameters as in Fig. 7.

antiferromagnetic correlations mediate the ferromagnetic correlations between two f orbitals and the ferromagnetic correlations between the conduction orbitals $(l,1)$ and $(l+1,1)$. The reduction of these two antiferromagnetic correlations will destabilize the FM state. As a result, the FM state transits to the AF state at the critical value V_c .

In the strong hybridization and strong coupling regime,¹⁵ the one-dimensional PAM has ferromagnetic ground state for the electron density between half and three-quarters fillings. It is interesting to compare the present result with it. In the one-dimensional PAM, for infinite U and $t \ll V$, the ferromagnetism requires $|\epsilon_f| \leq V$. At the exact half-filling case, the total spin per site is zero. However, in the present PALM, the ground state is ferromagnetic for $\epsilon_f \sim -U/2$ in the strong hybridization and half-filling case. The infinite U is not required as in Ref. 15. In the infinite U and $t \ll V$ limit, the ferromagnetism needs the infinite $\epsilon_f (\sim -U/2)$. The mechanisms of ferromagnetism for these two models are also different. In the one-dimensional PAM, the microscopic mechanism of the ferromagnetic ground state is similar to the one found by Nagaoka.² The coherent propagation of the Kondo singlet is responsible for the polarization of the spins. In the present PALM, the ferromagnetism results from the antiferromagnetic correlations between the nearest-neighbor sites. For infinite U and $t \ll V$, the mechanism of the ferromagnetism is similar to those proposed by Lieb³ and Tian and Lin¹⁹ in the Hubbard model for symmetric bipartite lattice.

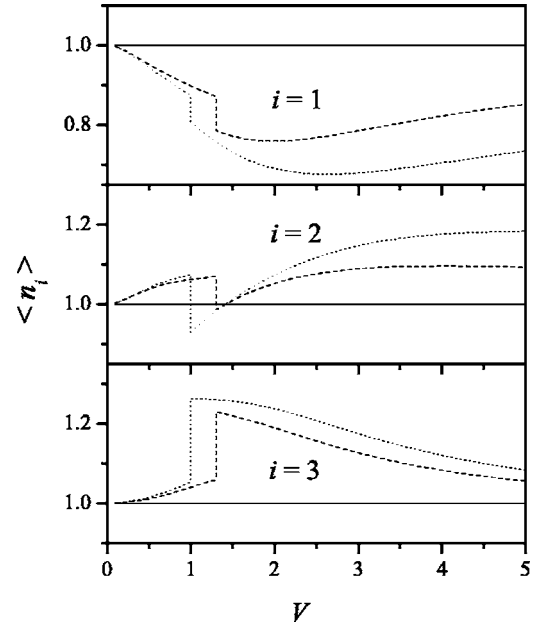


FIG. 9. Charge density $\langle n_i \rangle$ at site (l,i) for the same parameters as in Fig. 7.

In summary, we have studied the quasi-one-dimensional periodic Anderson-like chain at half-filling using the ED technique and the HFA. For the symmetric case, the ground state is always ferrimagnetic with spin $S = \frac{1}{2}$ per unit cell. In the weak hybridization case, the ferromagnetism originates from the ferromagnetic correlation between two f orbitals while in the strong hybridization case, the ferromagnetism is mainly contributed by the ferromagnetic correlation between the conduction orbitals $(l,1)$. In the large- V limit, the conduction orbitals $(l,1)$ form a spin- $\frac{1}{2}$ ferromagnetic chain with exchange decoupling from another conduction orbital $(l,2)$ and the f orbitals. For the asymmetric case, we construct the phase diagram. For given U and V , there are two critical values $0 > \epsilon_f^- > -U/2$ and $\epsilon_f^+ = -U - \epsilon_f^-$. The region between two critical values is the FM phase. Outside this region, the ground state is antiferromagnetic. With increasing U and V , the upper critical point ϵ_f^- decreases. In the large- V limit, the FM state exists only along the line $\epsilon_f = -U/2$ because of $\epsilon_f^- \rightarrow -U/2$. We find that in the weak coupling and strong hybridization case, the results by the HFA and the ED are consistent quantitatively.

ACKNOWLEDGMENTS

This work was supported by the National Natural Science Foundation of China under the Grants No. 50573059 and 10374073, and FANEDD of China under Grant No. 200034.

*Corresponding author. Email address: wzwang@whu.edu.cn

¹J. Hubbard, Proc. R. Soc. London, Ser. A **266**, 238 (1963).

²Y. Nagaoka, Phys. Rev. **147**, 392 (1966).

³E. H. Lieb, Phys. Rev. Lett. **62**, 1201 (1989).

⁴P. W. Anderson, Phys. Rev. **124**, 41 (1961).

⁵K. Ueda, H. Tsunetsugu, and M. Sigrist, Phys. Rev. Lett. **68**, 1030 (1992).

⁶G. S. Tian, Phys. Rev. B **50**, 6246 (1994).

- ⁷R. Jullien and R. M. Martin, Phys. Rev. B **26**, 6173 (1982).
- ⁸P. Santini, L. C. Andreani, and H. Beck, Phys. Rev. B **47**, 1130 (1993).
- ⁹J. Callaway, J. W. Kim, L. Tan, and H. Q. Lin, Phys. Rev. B **48**, 11545 (1993).
- ¹⁰R. Blankenbecler, J. R. Fulco, W. Gill, and D. J. Scalapino, Phys. Rev. Lett. **58**, 411 (1987).
- ¹¹C. D. Batista, J. Bonca, and J. E. Gubernatis, Phys. Rev. Lett. **88**, 187203 (2002); Phys. Rev. B **68**, 214430 (2003).
- ¹²M. Guerrero and R. M. Noack, Phys. Rev. B **53**, 3707 (1996).
- ¹³M. Guerrero and R. M. Noack, Phys. Rev. B **63**, 144423 (2001).
- ¹⁴M. Guerrero and C. C. Yu, Phys. Rev. B **51**, 10301 (1995).
- ¹⁵C. D. Batista, J. Bonca, and J. E. Gubernatis, Phys. Rev. B **68**, 064403 (2003).
- ¹⁶Y. Luo and N. Kioussis, Phys. Rev. B **65**, 195115 (2002).
- ¹⁷Y. V. Korshak, T. V. Medvedera, A. A. Ovchinnikov, and V. N. Spector, Nature (London) **326**, 370 (1987).
- ¹⁸W. Z. Wang, Z. L. Liu, and K. L. Yao, Phys. Rev. B **55**, 12989 (1997).
- ¹⁹G. S. Tian and T. H. Lin, Phys. Rev. B **53**, 8196 (1996).
- ²⁰H. Q. Lin and J. E. Gubernatis, Comput. Phys. **7**, 400 (1993).
- ²¹H. Tsunetsugu, M. Sigrist, and K. Ueda, Phys. Rev. B **47**, R8345 (1993).
- ²²M. Takahashi, *Thermodynamics of One-Dimensional Solvable Models* (Cambridge University Press, Cambridge, UK, 1999).